Combining Acoustic Emission Locations and a Microcrack Damage Model to Study Development of Damage in Brittle Materials*

David J. Holcomb, Charles M. Stone and Laurence S. Costin
Sandia National Laboratories, Albuquerque, NM 87185

SAND--89-2913C

DE90 005195

ABSTRACT: Under compressive stresses, brittle polycrystalline materials fail as the result of the growth, interaction and coalesence of microcracks. To predict the deformation of damaging material, constitutive laws developed for such materials must incorporate the effects of crack size, density, orientation, and interaction. A method of incorporating the accumulation and growth of microcracks into a continuum model is to use a measure of microcrack growth and interaction defined as damage. Although a number of damage theories have been proposed, there is no generally accepted experimental technique for detecting and measuring damage. Acoustic emissions (AE) have been correlated with microcrack nucleation and growth. We propose that AE locations and density are useful measures of damage that can be correlated with calculated damage. Our approach is to use acoustic emissions (AE) and computer modeling to study the development of damage in geomaterials.

1 BACKGROUND

Understanding and predicting the deformation and failure of rock under complex stress states requires taking account of the changes in mechanical properties that occur as damage accumulates in the material. A number of theories have been developed to incorporate damage into constitutive models (for example Kachanov 1986, Krajcinovic and Fonseka 1981, Costin 1983, and Singh and Digby 1989). Defining and measuring damage has proved to be a difficult task, with no standard method having emerged. Various measures have been proposed using unrecovered strain (Spooner and Dougill 1975), void density (Kachanov 1986) and AE activity (Holcomb and Costin 1986). A damage measure based on AE activity is appealing because it is easy to quantify the amount of AE as a function of test history. Other proposed measures can only be determined post-test making it impossible to determine when the damage occurred. In brittle materials, the processes that produce AE, such as pore collapse, microcrack growth and grain boundary slip, are all readily accepted as damage. Thus it is inviting to connect damage with AE activity.

Using AE activity as a measure of damage simplifies another major problem associated with damage theories: testing the theory. Many damage mechanisms are inherently anisotropic due to the extended planar nature of the voids or cracks being produced. Theories are usually developed using highly symmetrical tests, such as the conventional

*This work performed at Sandia National Laboratories supported by the U.S. Department of Energy under contract number DE-AC04-76DP00789.

---

triaxial test, for guidance. However, to be useful, the theories must allow for general stress states and inhomogeneous loading. Determining whether the predicted damage occurs under such conditions is difficult or impossible with most techniques. AE techniques are useful in these conditions because information about the damage process is transmitted by stress waves to the specimen surface where it is easily collected. By recording and analyzing AE signals from an array of transducers, the spatial and temporal development of damage can be followed in detail.

The purpose of this paper is to outline a general approach to the problem of verifying damage models. We propose the combined use of acoustic emissions and computational results as a way of testing analyses of rock behavior when significant damage is induced. The computations are based on a microcrack model of damage in brittle materials (Costin 1983) developed from triaxial test data. By associating the calculated damage with acoustic emissions (AE), the validity of the damage model under non-triaxial stress states can be checked. AE has already been used to test the predictions of Costin's damage model. Holcomb and Costin (1986) used the Kaiser effect to demonstrate the existence of an anisotropic damage surface, analogous to a yield surface, for material subjected to a uniaxial prestress. However the detailed predictions of the model have never been tested in a stress state more general than triaxial. As an example, we will present calculations of damage around a simulated borehole and compare the calculated damage patterns with AE locations. The intent is not to focus on the problem of borehole stability, but rather to demonstrate how AE can be used to judge the validity of a computed damage model.

2 DESCRIPTION OF EXPERIMENT

To investigate the correspondence between AE locations and damage calculated using the microcrack damage model, an experiment was performed using a parallelepiped of granite (200 by 200 by 94 mm) with a 16 mm diameter hole cored parallel to the largest face and loaded along an axis perpendicular to the hole axis. Eight piezoelectric transducers were mounted on the unloaded faces of the block along with two strain gages (Figure 1). This sample design was selected for a number of reasons. The two-dimensional nature of the loading is computationally tractable, but adjacent to the hole there is a stress concentration and gradient that makes the damage computation non-trivial. For an applied compressive stress $-\sigma$, the vertical stress at the side of the hole reaches a value of -3σ, which is the classic result for the stress concentration around a hole in an infinite solid under uniform uniaxial stress. The tangential stress at the top of the hole is equal to the applied stress but the sign is reversed which corresponds to a local zone of tensile stress, σ. The computation of damage around a hole in a stressed rock is of interest to the problem of stability of boreholes and underground openings.

A waveform acquisition system was used to capture AE events for later location and comparison with the calculated damage. AE events were recorded during loading to about 33% of the uniaxial strength of the granite. Owing to the stress concentration around the hole, it was expected that rock close to the hole would be near failure at the maximum applied load. Little hysteresis was observed by the strain gages, all of which were some distance from the hole, indicating that globally, only minor damage was done to the block. AE activity was brisk however, with several thousand events being detected. Speed limitations in the recording system prevented recording more than about 10% of the events.

Events were located, post-test, using a combination of the standard least squares technique and manual processing. Events were evenly distributed along the length of the hole, but were distinctively clustered when plotted in the plane perpendicular to the hole.

At each stage, the location algorithm placed several events in the hole, indicating that the location errors could be as large as 6-7 mm. More typical event timing residuals were less than 0.5 μsec, indicating location accuracies of about 3 mm. The location array had a blind spot at the sides of the hole. In these locations only 3 or 4 transducers could detect an event, as the ray paths to the transducers on the opposite face were blocked by the hole. For an acceptable location, a minimum of 5 transducers had to record the event. Thus no events could be located near the side of the holes. For events near the top and bottom of the hole, some transducers could be screened or waveforms distorted by the proximity of the free surface, leading to poor locations.

3 CONSTITUTIVE MODEL

The damage model for brittle materials used in this work is based on the work of Costin (1983) which accomodates the nucleation, growth, and coalesence of microcracks under compressive loading. In addition, the model allows for interaction among neighboring microcracks which leads to subsequent material failure or softening. There are several parts which make up this model. The crack growth criterion is based on elastic fracture mechanics concepts where the stress intensity factor at the crack tip, K_I, is a parameter that describes the state of stress at the crack tip. When K_I reaches a critical value, K_{Ic}, the crack extends until $K_I \leq K_{Ic}$. For modeling, the microcracks are assumed to be penny-shaped with crack radius a. The orientation of the crack surface, $\mathbf{n}$, allows us to define a crack vector, $\mathbf{a} = a\mathbf{n}$. Crack growth is driven by local tensile fields induced by material inhomogeneity. For a single crack with orientation $\mathbf{n}$ subjected to applied stress $\mathbf{T}$, the stress intensity at the crack tip is

$$K_I = \frac{2}{\pi}\sqrt{\pi \mathbf{a}\cdot\mathbf{n}}\left[\frac{tr\mathbf{T}}{3} + \mathcal{F}\left(\mathbf{a},\mathbf{n},d,d_1\right)\mathbf{n}^T\cdot\mathbf{T}'\cdot\mathbf{n}\right] \tag{1}$$

where the two terms in square brackets are the contributions of the hydrostatic and deviatoric components, $\mathbf{T}'$, of the applied stress. The function, $\mathcal{F}$, relates the applied deviatoric stress to a local tensile stress. $\mathcal{F}$ is a function of crack size and orientation and two microstructural lengths d and d_1. The size of the inhomogeneity-induced tensile fields is given by d, which is on the order of the grain size. Crack interaction effects are assumed to occur between cracks separated by a distance $d_1 > d$.

Provided that crack growth is stable, it is possible to represent the state of cracking by a function, $a(\theta,\phi)$, which represents the length of cracks with normals defined by the angles (θ,ϕ). A preexisting isotropic crack population is assumed. A damage vector, $\mathcal{D}_i$, defined as

$$\mathcal{D}_i = \frac{1}{a_o}\int_\Omega \mathbf{e}_i\cdot(\mathbf{a}-\mathbf{a}_o)H[K_I(\mathbf{n})]d\Omega \tag{2}$$

represents the combined effects of the crack population. In equation (2), $\mathbf{e}_i$ is a unit vector in the i^{th} coordinate direction, $\mathbf{a}_0$ is the initial crack length, and Ω implies integration over the upper unit hemisphere. Through the use of the function $H[K_I(\mathbf{n})]$, defined as

$$H[K_I(\mathbf{n})] = \left\{\begin{matrix}1\\0\end{matrix}\right\} \quad if \quad \left\{\begin{matrix}K_I > 0\\K_I \leq 0\end{matrix}\right\}, \tag{3}$$

only those cracks currently participating in the damage process are accounted for in the calculation of $\mathcal{D}_i$.

The final part of the model is the constitutive equation relating the strains to the imposed stresses and the state of damage. Assuming the matrix remains elastic, the

strains may be derived from an energy function in a manner similar to that described by Krajcinovic and Fonseka (1981). The compliance matrix is given by

$$S_{ijkl} = \frac{1+\nu}{E}\delta_{ik}\delta_{jl} - \frac{\nu}{E}\delta_{ij}\delta_{kl} + C_1(\delta_{ij})(\mathcal{D}_i\mathcal{D}_l\delta_{jk} + \mathcal{D}_j\mathcal{D}_k\delta_{il}) - C_2(\delta_{ij})(\mathcal{D}_i\mathcal{D}_j\delta_{kl}) \qquad (4)$$

where E and ν are the elastic constants for the undamaged material and C_1 and C_2 are additional constants that account for the effect of crack damage on the deformation. Equations (1), (2) and (4) are solved by an iterative procedure..

The microcrack damage model was implemented in the form of a material subroutine in the finite element code SANCHO (Stone et al. 1985). SANCHO is a special purpose code designed to compute the quasistatic, large deformation, inelastic response of planar or axisymmetric solids. A constant bulk strain, bilinear displacement isoparametric element is used for the spatial discretization. A self-adaptive dynamic relaxation scheme based on central difference pseudo-time integration and artificial damping is used to generate the series of equilibrium solutions.

In developing the two-dimensional finite element model for the Westerly granite block, we took advantage of the geometric symmetry and symmetry of loading by using a quarter-symmetry model. The symmetry conditions were enforced through the use of kinematic boundary conditions along the symmetry planes. The model was loaded by specifying a downward displacement of the top surface and the sides of the block were stress free. The final displaced state was achieved in 100 uniform displacement increments. Material constants used for the Westerly granite were those measured on the test block.

5 COMPARISON OF EXPERIMENT AND MODEL

In order to more clearly distinguish the changes in areas of AE activity and damage accumulation, the data set was divided into three portions: 0 to 45 MPa, 45 to 55 MPa and 55 to 65 MPa. Computed incremental damage contours and AE locations are plotted in Figure 2, where damage is defined as the magnitude of the damage vector calculated from Eqn. 2. Damage contours presented correspond to the increase in damage occurring between the specified stress steps. To emphasize the material being damaged, only the contour corresponding to a damage increment of 0.001 is plotted. Thus the areas enclosed by the contours include essentially all rock predicted to be damaged during a given load interval.

Results for loading from 0 to 45 MPa are shown in Figure 2a. As the block was loaded, damage was computed to occur at the top of the hole within the tensile stress zone, at the sides of the hole where compressive stresses were high and in lobes at 45 degrees to the vertical axis. Damage levels are predicted to be low and indeed only a few AE events were recorded in this stress interval.

AE locations are not in particularly good agreement with the calculated damage zones for the low stress stage. The regions of tensile stress at the top and bottom of the hole are poorly delimited by the AE activity. Events are more widely scattered than the calculations predict. As discussed earlier, the damage indicated by the contour at the sides of the hole was undetectible by the array. Both the computed damage and the observed AE indicate that damage primarily occurred near the hole.

Figure 2b shows results for the 45 to 55 MPa stage. According to the damage computation, the damaged zone expanded along the axes at 45 degrees to the block's vertical axis. Computed damage growth was significant at the side of the hole due to the compressive stress concentration. AE locations are more diffuse than the damage contours would predict but there are indications of concentration of events in the 45 degree lobes.

AE activity is not symmetric with respect to the hole axis; more events were located at the right side of the block than at the left. This may be the result of asymmetric loading or varying sensitivity of the transducer array. AE rates were much higher in this 10 MPA stress interval than in the preceeding 45 MPa interval, in agreement with the enlarged zone of material that the calculation predicted was experiencing damage.

Upon further loading to 65 MPa, Figure 2c shows that the incremental damage at the top of the hole had become insignificant. The maximum damage increment was still occurring at the side of the hole. There was also an increase in size of the incremental damage zone as the damaged area near the side of the hole grew. The damage zones at 45 degrees to the hole axis expanded, forming wings of damage around the hole. AE events are clustered at the base of these wings with a diffuse halo of events farther out from the hole. Events were located at the top of the hole, indicating that the lack of events in this area (Figs. 2a and 2b) was not due to inability to detect events in this region. Highly damaged areas at the sides of the hole are conspicuous by the total absence of locatable events. Event distribution is very asymmetric at high stress (see Figure 2c).

6 DISCUSSION AND SUMMARY

Our purpose in this work was to show a general approach to the problem of studying damaging materials by analyzing the damage process around a non-uniformly stressed hole. Agreement between observation and model would imply not only that microcrack growth and interaction are being correctly calculated but that the definition of damage is appropriate. Ultimately, models will be used in situations where extensive damage and material degradation are predicted, but where experimental verification will be difficult. Agreement between observations and calculations for inhomogeneous general stress states is an important step in qualifying the material model. By comparing increments of computed damage and location and density of AE events it is possible to detect significant failings of the damage modeling process. In this brief study it is evident that Costin's model (1983) represents many of the observed features. Calculated and observed damage, the latter measured by AE location and density, were similar except for the asymmetry which we attribute to nonuniform loading. The predicted formation of lobes of damaged material at higher stresses can be observed in the AE locations. Highly damaged zones at the side of the rock were unobservable by the transducer array used. AE locations seemed to indicate a more diffuse cloud of activity than the model predicted, but from the limited number of events located, it is difficult to assess the significance of the difference. There did seem to be a clear discrepancy between predicted damage and AE activity in the tensile stress region at the top and bottom of the hole. As Figures 2a and b show, AE activity was initially sparse in this area and extended farther from the hole than predicted. For these stages, calculated damage was high and concentrated close to the hole. At the last stage (Fig. 2c), a number of events were observed in this region when the damage calculation indicted that little damage should be occurring. If repeated testing confirmed this result, then the model would have to be modified. Since the model was developed for use with compressive stress states, it would not be suprising if it required modification when applied to tensile stress fields. Several parameters in the model are not well known. Detailed knowledge of the damage distribution will help to constrain these parameters.

Improvements can be made in several areas. The damage computations provide a detailed picture of the damage process. To take advantage of this detail, many more AE events need to be recorded and located. The system used in the present test was only able to record about 10% of the events. A faster system or slower loading rates will be necessary to capture more events. Improvements in the transducer network can be

made based on pretest calculations. In areas of high damage, such as along the hole sides in this work, higher precision locations may be required to delineate levels of damage. If a significant portion of the ray paths from events to transducers will pass through a highly damaged zone, then it may be necessary to use a non-homogeneous velocity model to improve accuracy of the location process. One area not addressed here is the spatial orientation of microcracks. The microcrack damage model predicts in detail what crack orientations will grow. Focal mechanisms can be determined for individual AE events if signal quality is high and the crack orientation determined to lie on one of the nodal planes of the focal mechanism. Post-test, crack densities and orientations can be determined directly from thin sections.

REFERENCES

Costin, L. S. 1983. Damage mechanics in the post-failure regime. Mech. of Maters. 4:149-160.

Holcomb, D. J. and L. S. Costin 1986. Detecting damage surfaces in brittle materials using acoustic emissions. J. Appl. Mech. 108:536-544.

Kachanov, L. M. 1986. Introduction to continuum damage mechanics. Dordrecht: Martinus Nijhoff.

Krajcinovic, D. and G. Fonseka 1981. The continuous damage theory of brittle materials. J. App. Mech. 48:809.

Singh, U. K. and P. J. Digby 1989. A continuum damage model for simulation of the progressive failure of brittle rocks. Int. J. Solids and Struct. 25:647-663.

Spooner, D. C. and J. W. Dougill 1975. A quantitative assessment of damage sustained in concrete during compressive loading. Mag. of Concrete Res. 27:151-160.

Stone, C. M., R. D. Krieg and Z. E. Beisinger 1985. SANCHO- a finite element computer program for the quasistatic, large deformation, inelastic response of two-dimensional solids. Sandia National Laboratories Internal Report SAND84-2618.

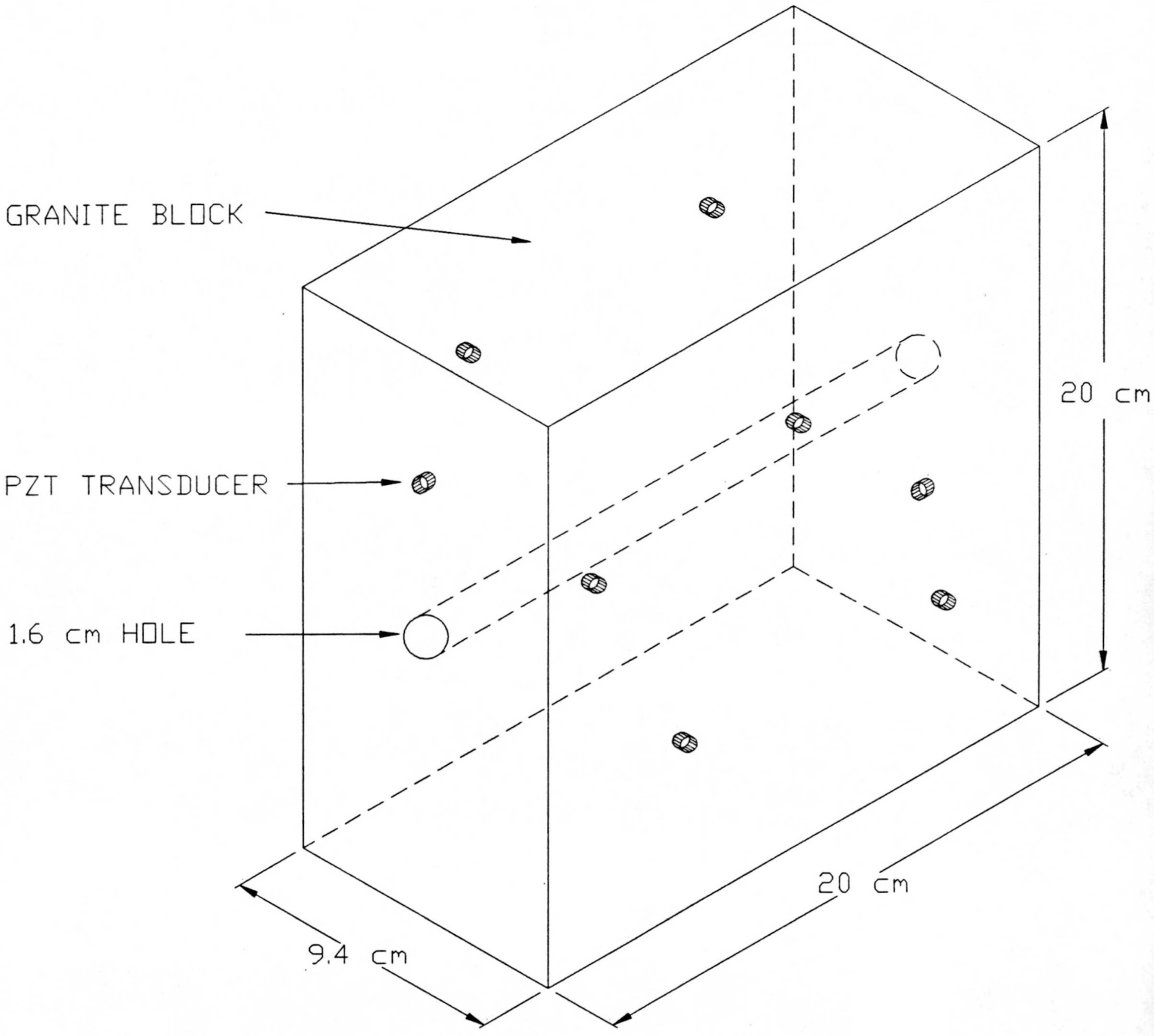

Figure 1. Diagram of sample showing transducer and strain gage locations.

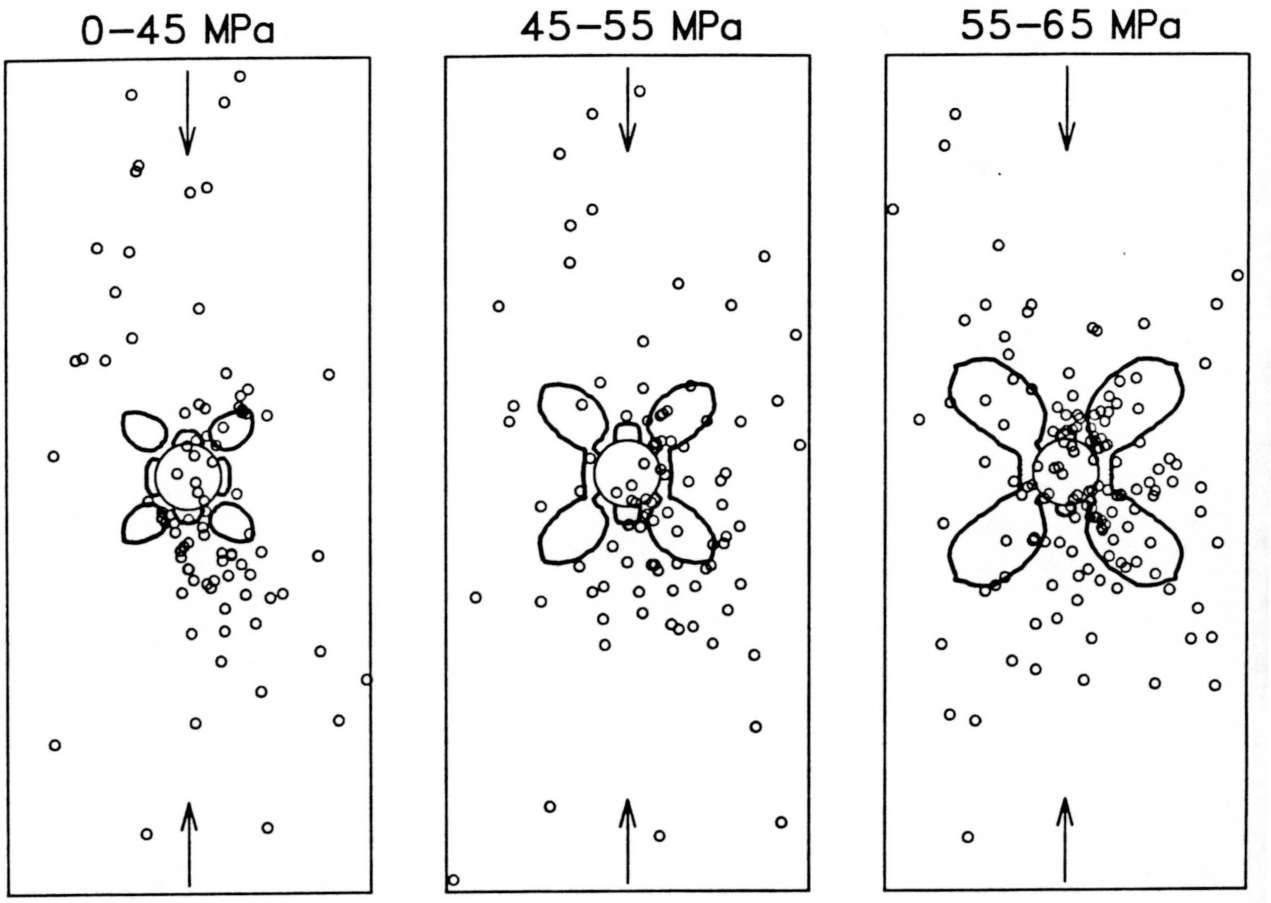

Figure 2. Locations for AE events occurring at stresses between (a) 0 and 45 MPa, (b) 45 and 55 MPa and (c) 55 and 65 MPa. A circle is plotted at each event location with the size of the circle corresponding to the location uncertainty as judged by the magnitude of the time residuals. Solid contours are the boundary of the zone where damage has occurred between the start and end of each step. Uniaxial load was applied along the axis indicated by the arrows.